Electronic Supplementary Material (ESI) for Journal of Materials Chemistry A.

Supporting Information

A well-designed water-soluble binder enlightening 5 V-class $LiNi_{0.5}Mn_{1.5}O_4$ cathodes

Tiantian Dong,[†] Huanrui Zhang,[†] Yue Ma, Jianjun Zhang, Xiaofan Du, Chenglong Lu, Xuehui Shangguan, Jiedong Li, Min Zhang, Jinfeng Yang, Xinhong Zhou, Guanglei Cui**

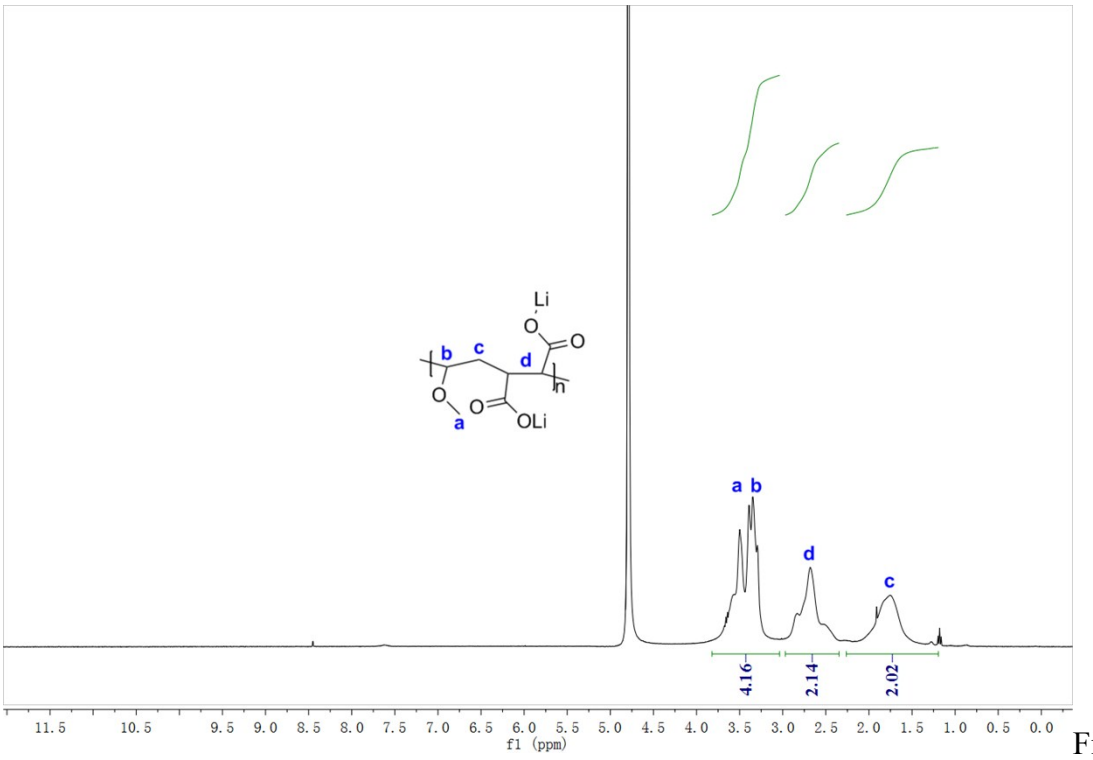

Figure S1. ^{1}H NMR spectra of P(MVE-LMA) binder in $^{d}DMSO$

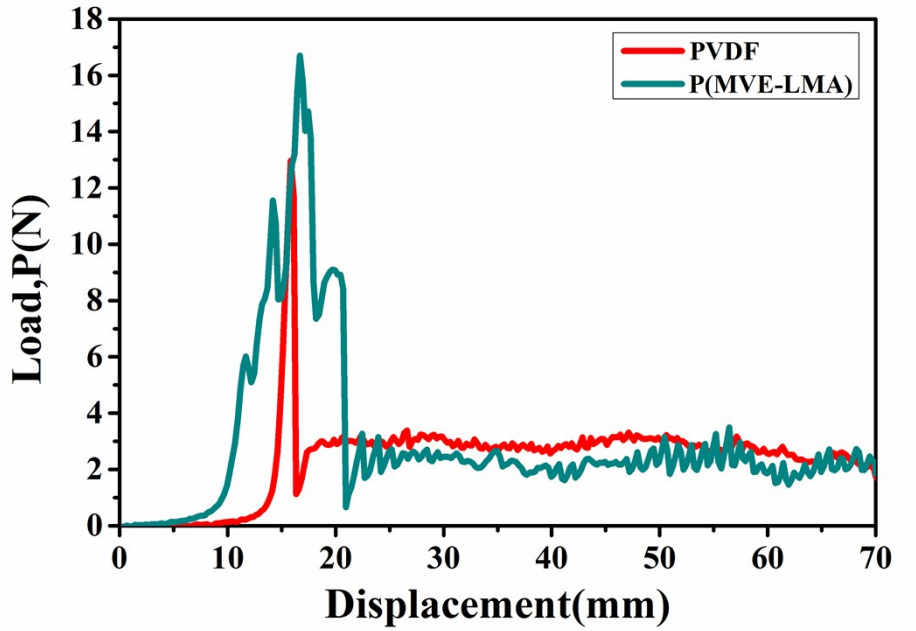

Figure S2. Peel-strength curves of the LNMO electrodes with PVDF and P(MVE-LMA) binder.

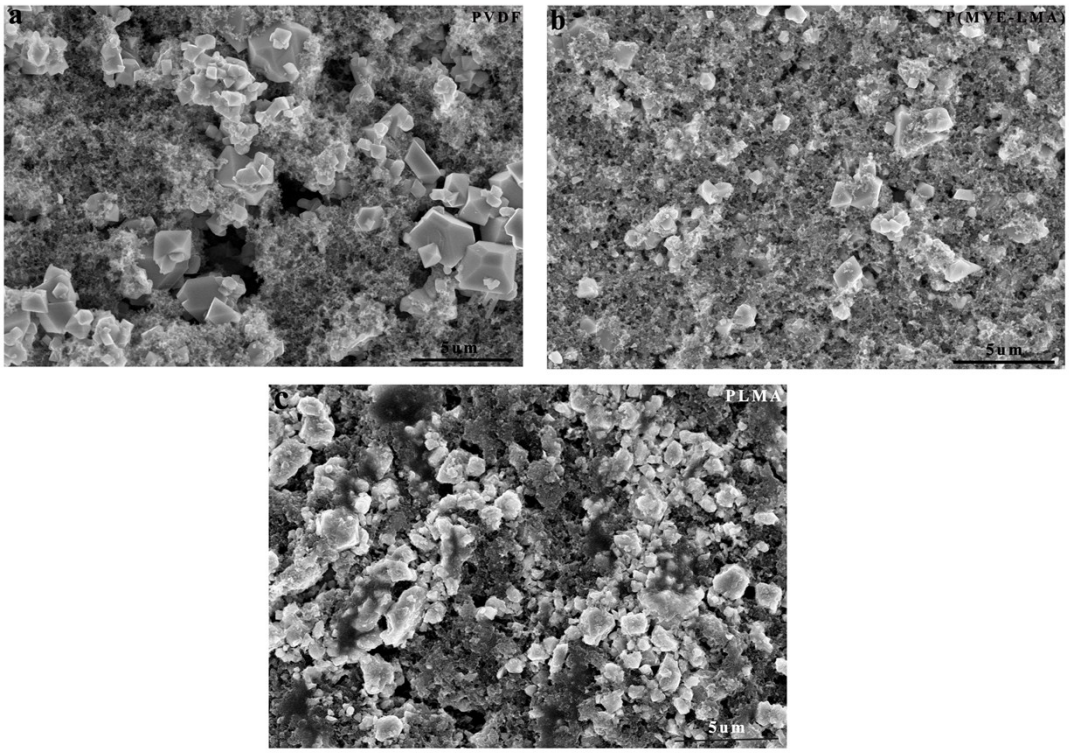

Figure S3. Typical SEM images of pristine cathodes with a) PVDF binder, b) P(MVE-LMA) binder, and c) PLMA binder.

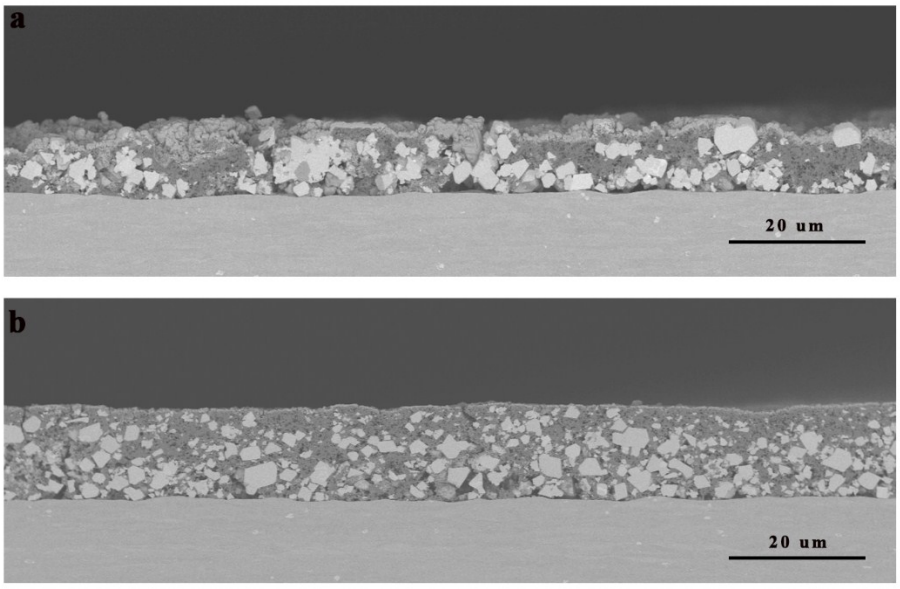

Figure S4. Sectional SEM image of pristine cathodes with a) PVDF binder, and b) P(MVE-LMA) binder.

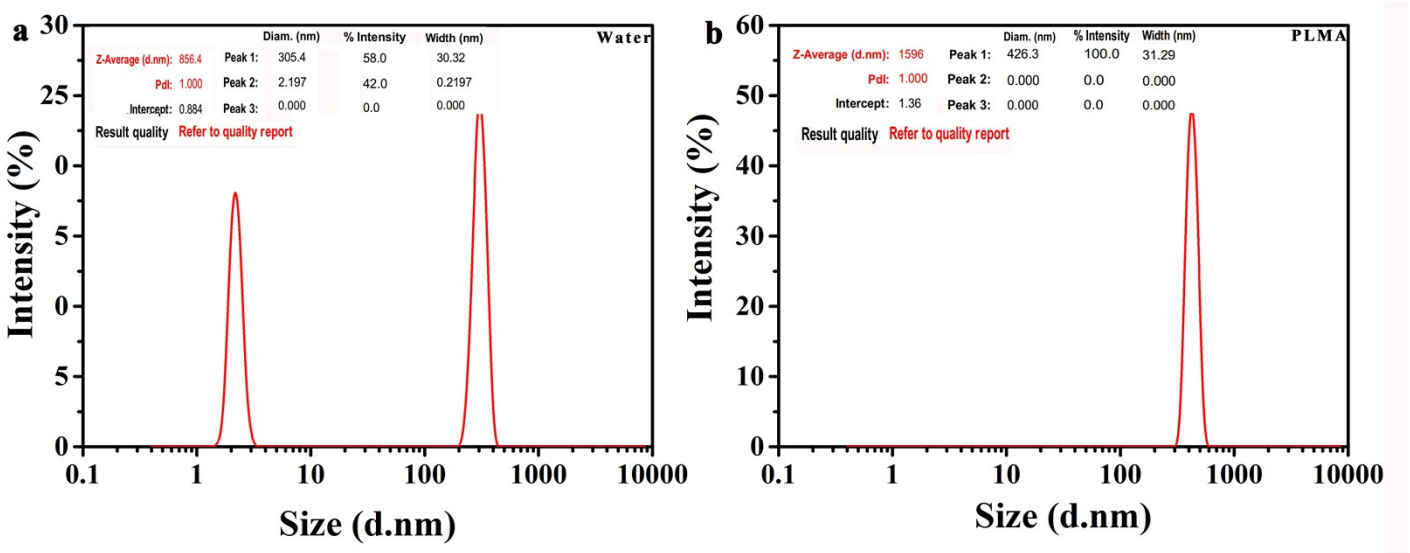

Figure S5. Particle sizes of a) water, and b) PLMA aqueous solutions.

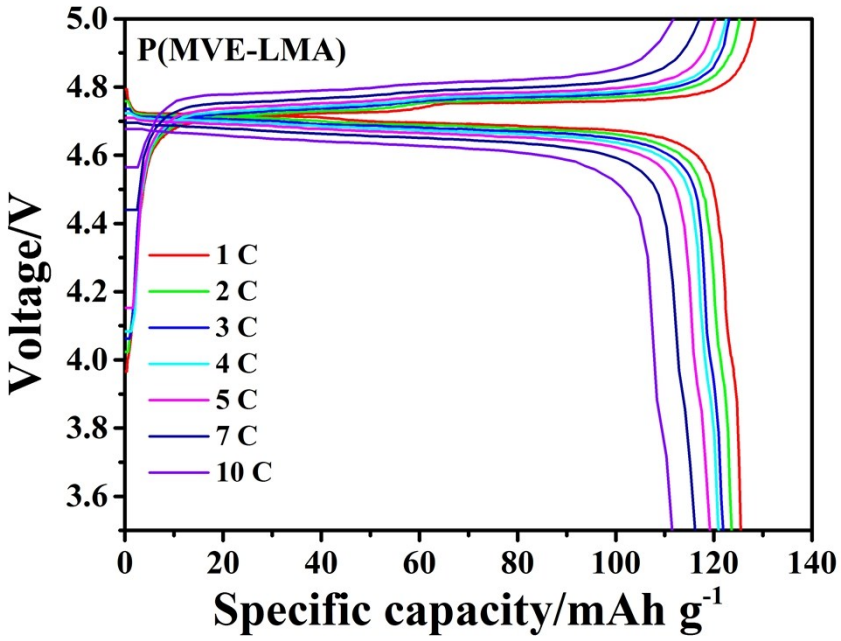

Figure S6.The corresponding discharge/charge profiles at different rates of LNMO electrodes with P(MVE-LMA) binder.

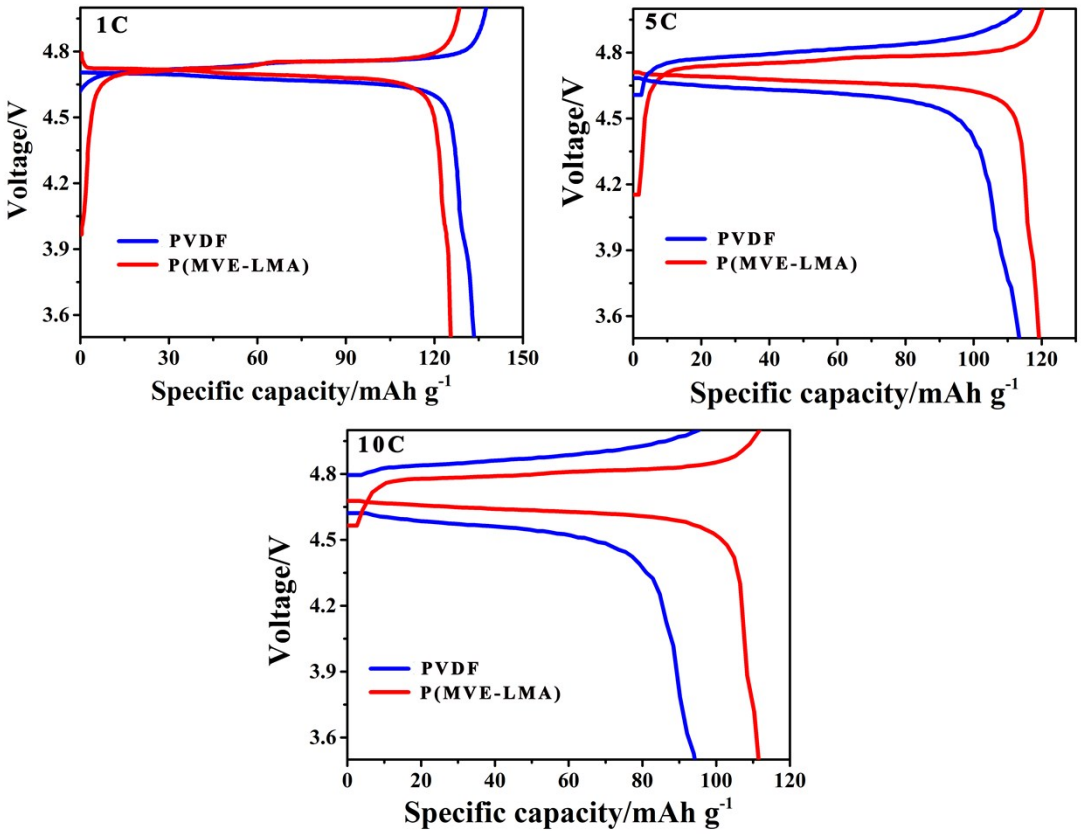

Figure S7. The discharge/charge profiles of LNMO electrodes with PVDF and P(MVE-LMA) binder at the rates of 1 C, 5 C and 10 C.

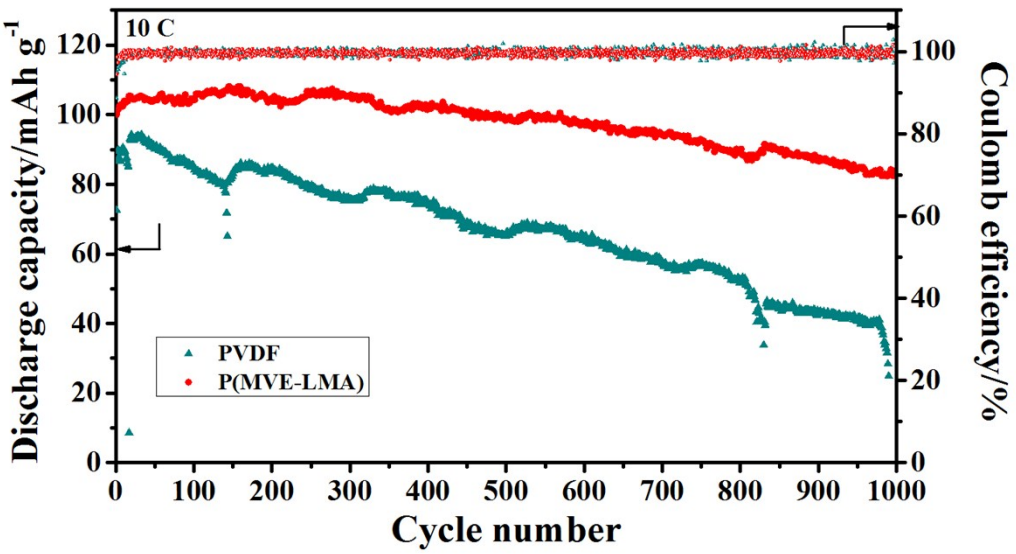

Figure S8. Long-term cycle performance and Coulombic efficiency of P(MVE-LMA) based LNMO electrodes at 10 C.

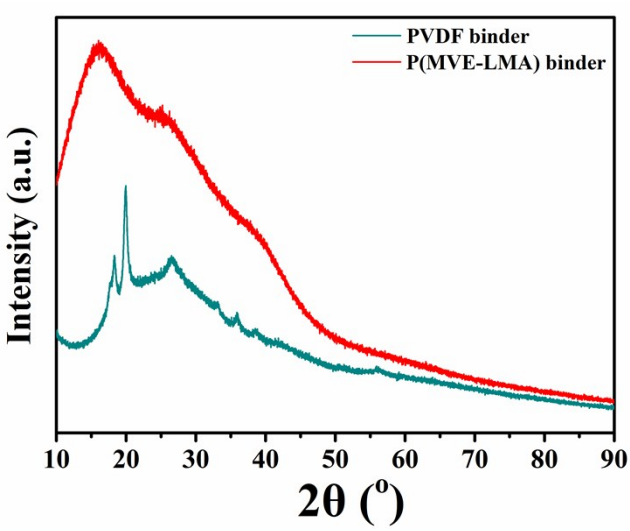

Figure S9. XRD patterns of PVDF and P(MVE-LMA) binder.

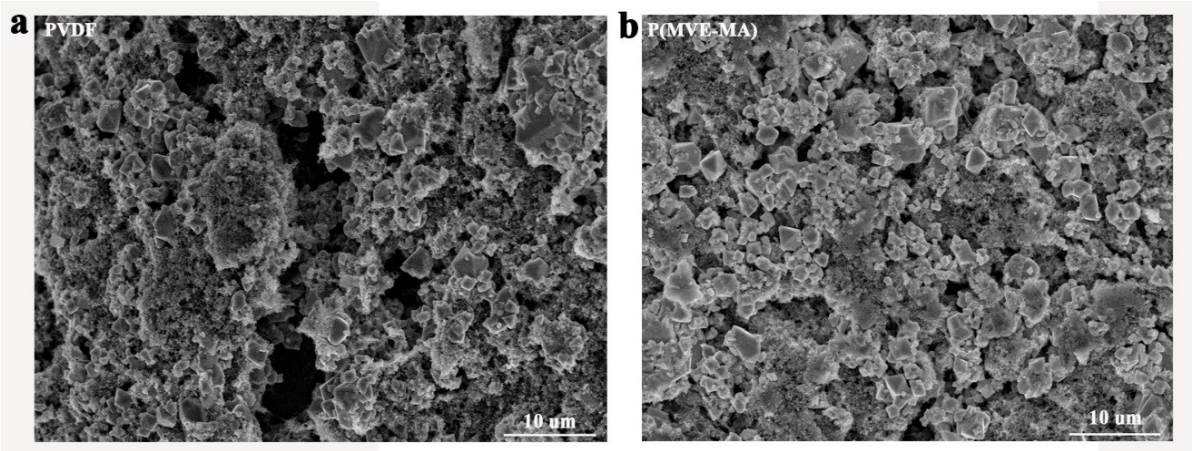

Figure S10. Typical SEM images of cycled LNMO electrodes with a) PVDF binder, and b) P(MVE-LMA) binder disassembled from LNMO/Li batteries after 100 cycles.

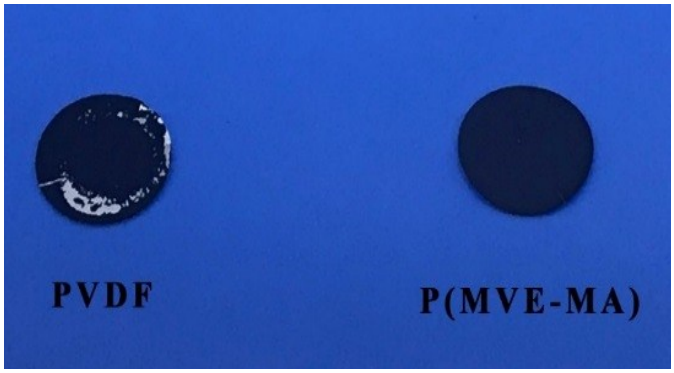

Figure S11. The digital photograph of LNMO electrodes disassembled from LNMO/Li batteries after 500 cycles.

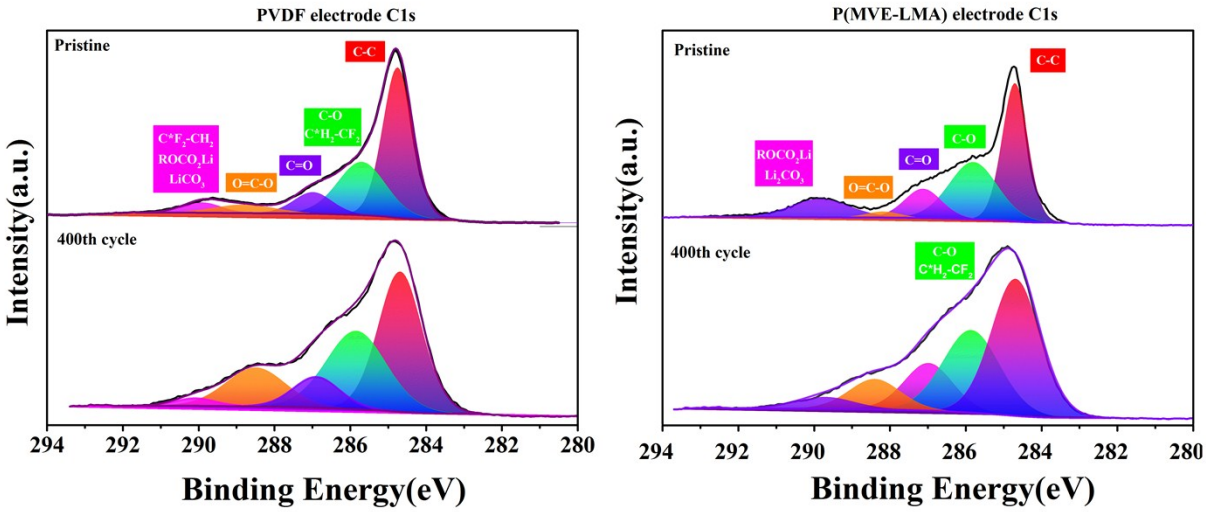

Figure S12. The surface composition of LNMO electrodes with PVDF and P(MVE-LMA) binders tested by high-resolution XPS measurements before and after cycling. The C 1s spectra of a) PVDF based LNMO electrodes and b) P(MVE-LMA) based LNMO electrodes.

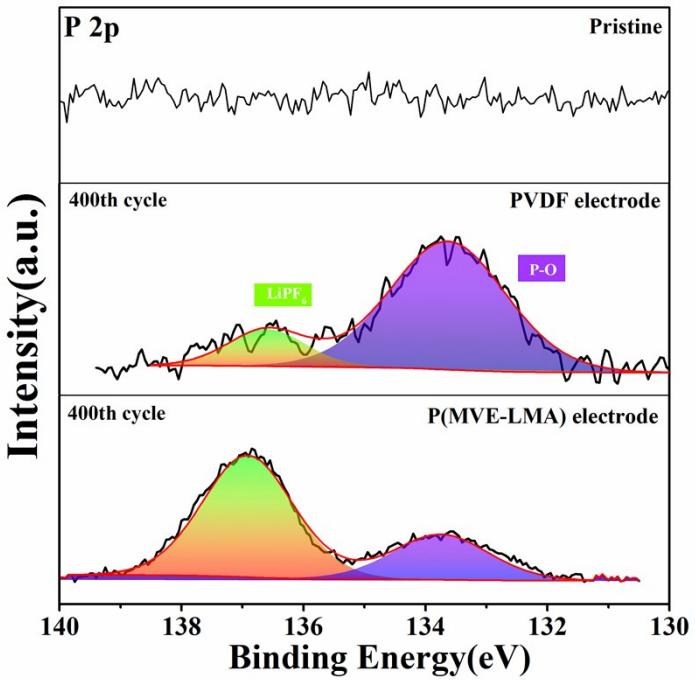

Figure S13. XPS spectra of P 2p of cycled LNMO cathode disassembled from the LNMO/Li half-cells with PVDF and P(MVE-LMA) binder.

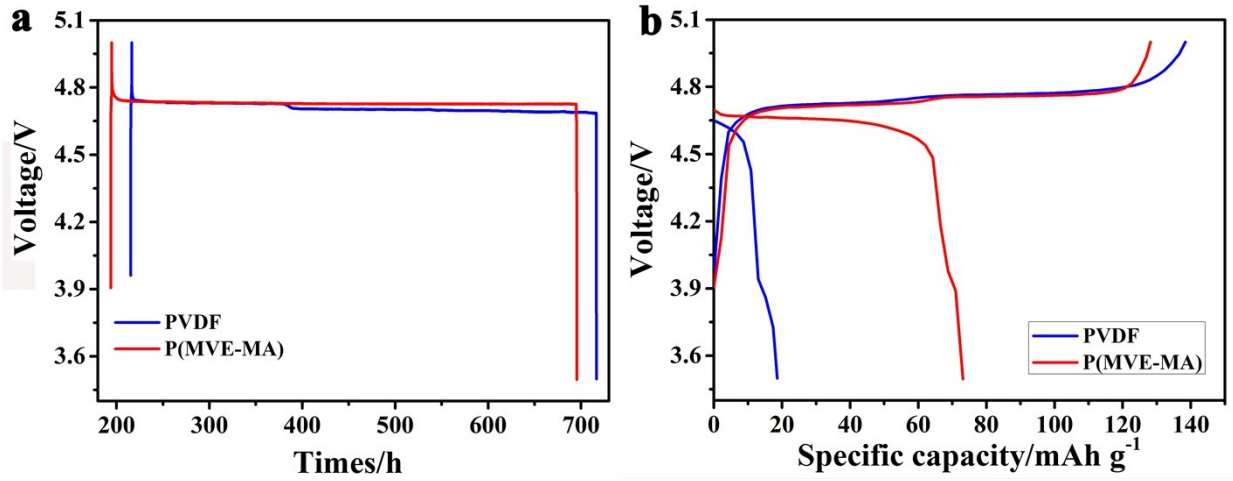

Figure S14. a) Voltage-time curves for self-discharge after 100 cycles and b) charge/discharge curves of LNMO electrodes with PVDF or P(MVE-LMA) binder at the 101th cycle.

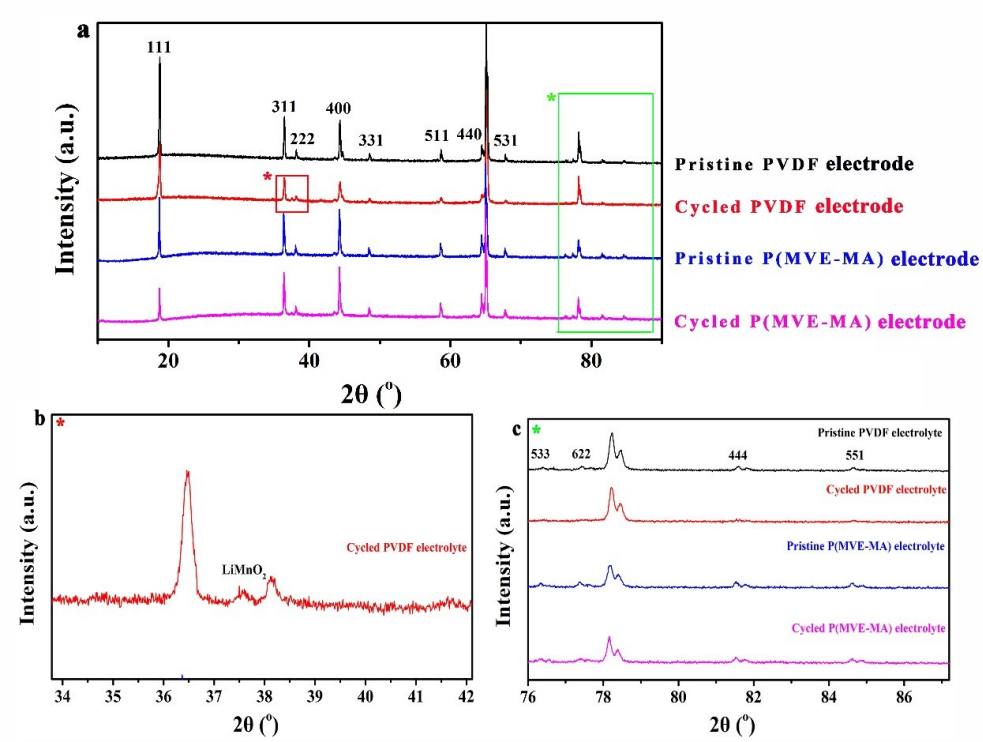

Figure S15. X-Ray diffraction patterns of a) pristine and cycled LNMO electrodes based on PVDF or P(MVE-LMA) binder. b) and c) were the corresponding selected regions.

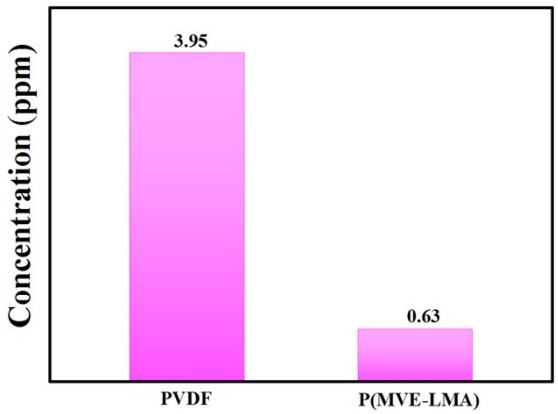

Figure S16. Inductively coupled plasma-optical emission spectrometer (ICP-OES) results of dissolution concentrations of Mn ions within cycled LNMO electrodes.

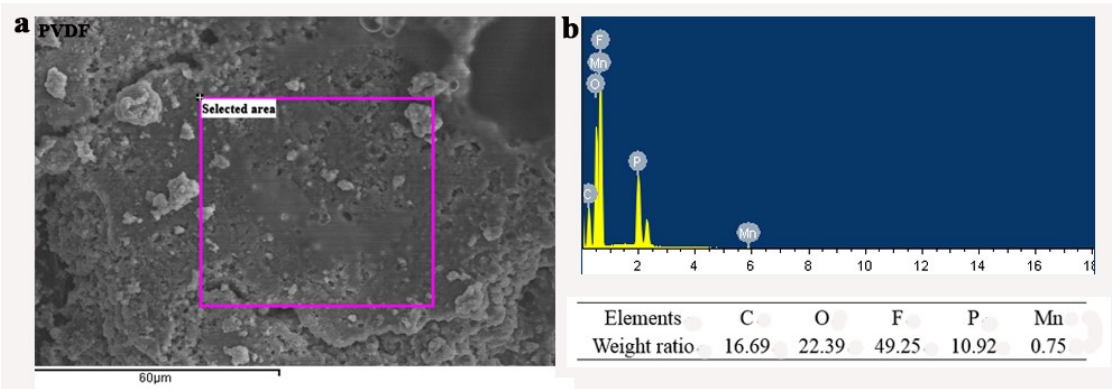

Figure S17. a) Typical SEM images of the Li metal anode disassembled from the LNMO/Li battery with PVDF binder after 100 cycles and b) the corresponding EDX results. Inset shows the specific weight ratio on the Li metal surface.

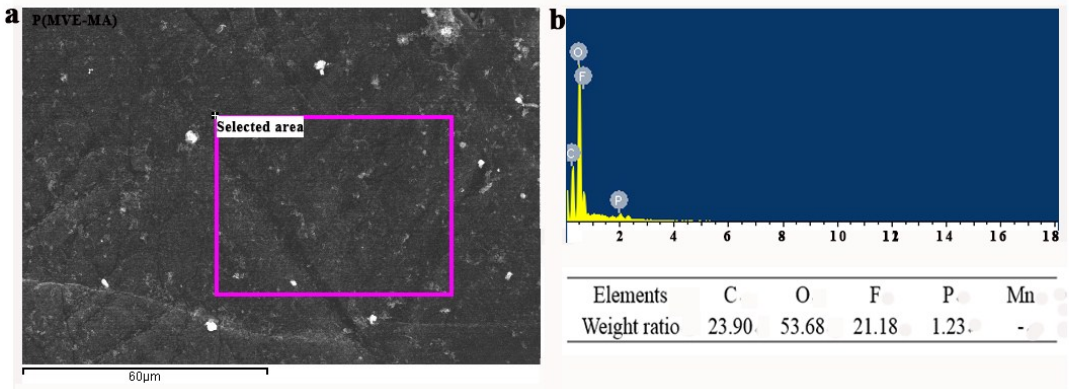

Figure S18. a) Typical SEM images of the Li metal anode disassembled from the LNMO/Li battery with P(MVE-LMA) binder after 100 cycles and b) the corresponding EDX results. Inset shows the specific weight ratio on the Li metal surface.

Table S1. Peak assignment of C 1s spectra.

Binding Energy (eV)	Peak assignment
290.7−290.9	$ROCO_2Li$, Li_2CO_3, $C^*F_2-CH_2$ (PVDF)
288.7−288.8	O=C−O
287.0−287.1	C=O
285.7−285.9	C-O, $C^*H_2-CF_2$ (PVDF)
284.8	C−C

Table S2. Peak assignment of O 1s spectra.

Binding Energy (eV)	Peak assignment
533.4−533.8	C−O
531.7	$ROCO_2Li$, Li_2CO_3, O=C−O, C=O
529.6−529.9	Lattice oxygen of $LiNi_{0.5}Mn_{1.5}O_4$

Table S3. Peak assignment of F 1s spectra.

Binding Energy (eV)	Peak assignment
687.8−688.5	$LiPF_6$, CH_2-CF_2 (PVDF)
685.5−687	$Li_xPO_yF_z$, Li_xPF_z and F−Li/Ni/Mn

Table S4. Peak assignment of P 2p spectra.

Binding Energy (eV)	Peak assignment
136.7−137.3	P−F
133.7−134.2	P−O

Table S5. Coordination energies of Mn atom with PVDF and P(MVE-LMA).

	P(MVE-LMA)	PVDF
	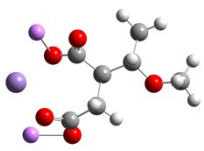	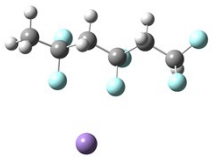
Ed(Ha)	−0.0327	−0.0174
Ed(eV)	−0.8903	−0.4746